Available online at www.sciencedirect.com
ScienceDirect
Chinese Journal of Aeronautics 23(2010) 109-116
Chinese Journal of Aeronautics
www.elsevier.com/locate/cja

Low C/N_0 Carrier Tracking Loop Based on Optimal Estimation Algorithm in GPS Software Receivers

Miao Jianfeng[a,b,*], Chen Wu[b], Sun Yongrong[a], Liu Jianye[a]

[a]*Navigation Research Center, College of Automation Engineering, Nanjing University of Aeronautics and Astronautics, Nanjing210016, China*

[b]*Department of Land Surveying and Geo-informatics, Hong Kong Polytechnic University, Hong Kong, China*

Received 16 July 2009; accepted 7 September 2009

Abstract

Suppressing jitter noises in a phase locked loop (PLL) is of great importance in order to keep precise and continuous track of global positioning system (GPS) signals characterized by low carrier-to-noise ratio (C/N_0). This article proposes and analyzes an improved Kalman-filter-based PLL to process weak carrier signals in GPS software receivers. After reviewing the optimal-bandwidth-based traditional second-order PLL, a Kalman-filter based estimation algorithm is implemented for the new PLL by decorrelating the model error noises and the measurement noises. Finally, the efficiency of this new Kalman-filter-based PLL is verified by experimental data. Compared to the traditional second-order PLL, this new PLL is in position to make correct estimation of the carrier phase differences and Doppler shifts with less overshoots and noise disturbances and keeps an effective check on the disturbances out of jitter noises in PLL. The results show that during processing normal signals, this improved PLL reduces the standard deviation from 0. 010 69 cycle to 0. 007 63 cycle, and for weak signal processing, the phase jitter range and the Doppler shifts can be controlled within ±17° and ±5 Hz as against ±25° and ±15 Hz by the traditional PLL.

Keywords: global positioning system; signal processing; Kalman filters; software radio; phase locked loop

1. Introduction

Software-defined radios (SDRs) have been around for more than ten years. As a global positioning system (GPS) software receiver, this technology was implemented by D. M. Akos in the GPS signal processing field in 1997[1]. It is a powerful tool for GPS researchers[1-3] because its ability to ame-liorate the low-level functionality of a GPS receiver without altering the physical hardware, and allows rapid testing of newly developed algorithms and to be used in a non-traditional way[3-4].

With the development of the GPS software receiver, processing low carrier-to-noise ratio (C/N_0) signals at a GPS software platform has attracted much more attention recently. As for acquisition of GPS weak signals, the main problem consists in the increase of integration time to reduce the ill effects of various noises. The simplest method is to combine the coherent and incoherent integrations[3, 5] and calculate with the fast Fourier transform (FFT) algorithm to increase the relative strength of signals from satellites[5]. The alternative half-bits method increases the integration time by performing two independent acquisition computations by using two alternative data sets, of which one is guaranteed to have no bit transitions[5]. The full-bits method involves the estimation of the data bit transition times[5-6].

The main approaches to enhance the performances to track low C/N_0 signals are to improve loop architectures and develop new filter algorithms[2, 7-8]. The GPS signal tracking is performed by the phase locked loop (PLL) for carriers and the delay locked loop (DLL) for codes. The main duty of these loops is to generate replicas of the incoming satellite signals for the receiver. For tracking weak carrier signals, the

*Corresponding author. Tel.: + 86-25-84892304-855.
E-mail address: dbqr@163.com
Foundation items: National Natural Science Foundation of China (40671155); National High-tech Research and Development Program of China (2006AA12A108); Research Program of Hong Kong Polytechnic University (G-U203)

doi: 10.1016/S1000-9361(09)60194-1

focus is laid on better PLL architecture and filter design to reduce various noises. Having analyzed the spectrum characteristics of various error sources, A. Razavi, et al.[8] elucidated the performances of various loop architectures in weak signal circumstances. F. Legrand, et al. [9] put forward a fast adaptive bandwidth PLL to reduce the effects of thermal noise. Special loop designs and algorithms were introduced to reduce the effects of multipath[10-11]. The assistance from other information and sensors is of great use in tracking weak signals. For example, the assisted-GPS (AGPS) technology uses the information about approximate positions of the receiver and satellite from other GPS receivers to help improve the loop's ability to track weak signals. Another example is to use other sensors, like inertial measurement unit (IMU), for estimating the Doppler shifts[12-13]. Although some researchers implement the Kalman filters in tracking loop, and process with simulated GPS data [14-15], they have not paid enough attention to the importance of suppressing the phase jitter noises in PLL.

This article suggests a Kalman-filter-based loop to track weak carrier signals. It begins with a review of statistics about total phase jitter noises of PLL, followed by establishing a standard Kalman-filter-based PLL by de-correlating the dynamic model noises and the measurements noises to improve the performances to track weak GPS signals. For the signals with normal C/N_0, the new PLL provides more stable and precise estimation of phase errors and Doppler shifts while for those with low C/N_0, it can keep effective check on the irregular phase jitter noises by correct estimation of the true phase differences between the replicas and the received signals. Finally, this article ends with performing experiments to provide results as the base for drawing conclusions. Compared with the traditional second-order PLL, the estimation-based method is more flexible and robust to tackle errors in GPS measurements.

2. Review of Traditional Second-order PLL and Analysis of Phase Jitter Noises

2.1. Second-order PLL in GPS software receiver

The most commonly used tracking method in GPS receivers contains two coupled carrier/CA signal tracking loops: the PLL and the DLL. In software receivers, this typical tracking algorithm is still in fashion, yet this article concentrates attention only on the PLL. For a GPS software receiver, the input signals are collected by the radio frequency (RF) front-end, which converts satellite RF signals into intermediate frequency (IF) signals and then samples the IF signals with an A/D converter. A model of the sampled IF signals can be simply expressed by[3]

$$S(t_k) = AD(t_k)C(t_k)\cos(\omega_{IF}t_k + \varphi_0) + e(t_k) \quad (1)$$

where $S(t_k)$ is the sampled signal at the sample time t_k; A the signal amplitude; $D(t_k)$ the navigation data stream; $C(t_k)$ the CA code; ω_{IF} the IF signal frequency; ϕ_0 the initial phase angle and $e(t_k)$ the noise.

To improve the performances of the GPS receivers with low C/N_0, the key is to design better tracking loops having better ability to subdue multisource noises. The carrier PLL includes three components:a phase detector, a loop filter ($F(s)$) and a voltage-controlled oscillator (VCO) (see Fig.1). Inputs to a PLL are received in the form of GPS continuous frequency-modulated signals with an input signal phase φ_i. The VCO is responsible for regenerating a replica signal with a phase φ_r, which changes after φ_i. If both are synchronous in the signal frequencies and the phases, the tracking loop is in a locking state.

Ideally, in a stable phase lock condition, the phase errors between the input and the replica ($\delta\varphi=\varphi_i-\varphi_r$) should be maintained around zero.

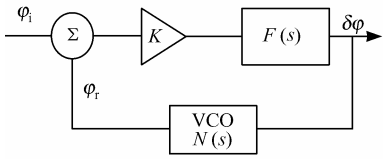

Fig.1 Diagram of a PLL.

The performances of a PLL mainly depend on the loop filter. For a traditional second-order PLL, the close-loop transfer function can be expressed by[3-4]

$$H(s) = \frac{2\zeta\omega_n s + \omega_n^2}{s^2 + 2\zeta\omega_n s + \omega_n^2} \quad (2)$$

where ω_n is the natural frequency, ζ the damping factor.

The phase error of the PLL(see Fig.1)can be expressed by

$$\delta\varphi = \varphi_i - \varphi_r = \delta\varphi_t + \delta\varphi_\varepsilon \quad (3)$$

where $\delta\varphi_t$ represents the true phase difference between the received GPS carrier phase and the locally generated one, $\delta\varphi_t$ the phase tracking jitter errors due to multisource noises, the errors caused by GPS satellite's and receiver's clock instability, ionosphere interferences, thermal noises, dynamic stresses, multipath and blockage interferences and otherwise.

2. 2. Analysis of PLL's total phase jitter errors

The total phase jitter noise is a reliable metric for

assessing the performances of the PLL to process low C/N_0 signals[4, 8]. As the amplitude of phase errors is closely linked to the PLL performances, the latter would be out of the locked state when the phase jitter error goes beyond a certain limit. Therefore, the knowledge of the characteristics of the phase jitter noise is of big help to the design of tracking loops[8].

To keep precise and continuous track of GPS carrier signals, the total phase jitter should be[4]

$$\sigma_\varphi = \sqrt{\sigma_w^{\ 2} + \sigma_c^{\ 2}} + \frac{\sigma_d}{3} \le 15° \tag{4}$$

where σ_φ represents the total phase jitter in PLL, σ_w^2 the phase jitter due to white noises, σ_c^2 the phase jitter due to related or colored noises and σ_d the dynamic stresses caused by the tracking loop failing to give quick responses to abrupt phase changes.

Let tan^{-1} be the phase discriminator (PD) and B_n the tracking loop bandwidth, then σ_w^2 can be defined as[8]

$$\sigma_w^2 = \frac{B_n}{C/N} \tag{5}$$

and the phase jitter caused by colored noises can be determined by[8]

$$\sigma_c^2 = \int_0^\infty \left\| H_e(f) \right\|^2 G_c(f)\,df \tag{6}$$

where the error transfer function $H_e(f)$ is fixed by 1-$H(f)$ and $G_c(f)$ is the one-sided power spectral density(PSD)of colored noise sources.

Detailing the sources of the phase jitter caused by colored noises, Eq. (6) can be rewritten into[8]

$$\sigma_{rx}^2 + \sigma_{sv}^2 + \sigma_v^2 + \sigma_a^2 = \int_0^\infty \left\| H_e(f) \right\|^2 [G_{rx}(f) + G_{sv}(f) + G_v(f) + G_a(f)]\mathrm{d}f \tag{7}$$

where $\sigma_{rx}^2, \sigma_{sv}^2, \sigma_v^2$ and σ_a^2 and σ_a^2 separately represent the error sources from jitters of receiver clock phase, satellite clock phase, vibration-induced phase and phase due to atmospheric effects with $G_{rx}(f), G_{sv}(f), G_v(f)$ and $G_a(f)$ being their corresponding PSDs. Modeling of the above phase jitter caused by color noises needs lots of statistical information and a prior knowledge. This article only cites the representative point, further more details, readers may refer to Ref. [4] and Ref. [8].

The errors caused by dynamic stress phase jitters can be derived with the steady state error formulas[4]. The dynamic stress error from the second-order PLL can be expressed by

$$\sigma_d = \frac{\mathrm{d}^2R/\mathrm{d}t^2}{\left(B_n/0.53\right)^2} = 0.280\,9\frac{\mathrm{d}^2R/\mathrm{d}t^2}{B_n^2} \tag{8}$$

where $\mathrm{d}^2R/\mathrm{d}t^2$ represents the acceleration between the GPS receiver and satellite.

Based on all the above-discussed jitter components, substituting Eq.(5)-Eq.(8) into Eq.(4), the total jitter can be obtained

$$\sigma_\varphi = \sqrt{\sigma_w^2 + \sigma_{rx}^2 + \sigma_{sv}^2 + \sigma_v^2 + \sigma_a^2} + 0.09363\frac{\mathrm{d}^2R/\mathrm{d}t^2}{B_n^2} \tag{9}$$

By using the above-cited equations as well as the empirical statistic models[8], the total phase jitter can be approximately estimated. In a traditional second-order PLL with a certain C/N_0, the white noise phase jitter σ_w^2 monotonously increases while the other components decrease with the loop bandwidth rising. Therefore, it is possible to find out an optimal bandwidth that can minimize the total phase jitter noises (see Eq. (9)). Based on the colored noise models[8, 13] and the total phase jitter definition[4], the optimal bandwidth for the traditional second-order PLL has been calculated to be 7-10 Hz for the C/N_0 ranging from 20 to 25 dB-Hz(see Fig.2).

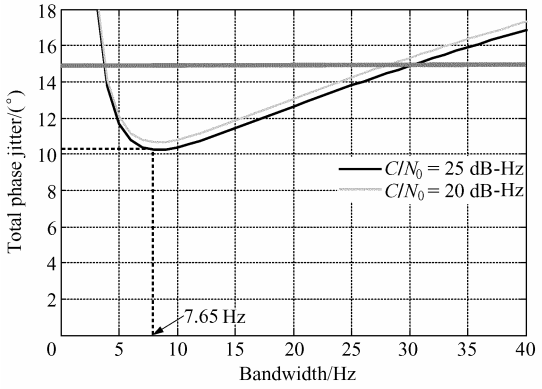

Fig.2 Weak signal total phase jitter vs bandwidth.

3. Design of a Kalman-filter-based PLL

The key problem for a PLL is precise estimation of the phase errors in the existence of multisource noises in order for the replica carrier outputs from the VCO to match the input phase. The above-discussed second-order PLL only provides the precise phase errors with the optimal bandwidth when the jitter noises strictly follow the statistical models in Eq. (9).

However, in the case of weak signals, there are many unstable phase jitters from, for instance, the ionospheric scintillations and multipath effects that might exert influences upon GPS signals. These jitters are difficult to model precisely due to their instinctive nature and complex mechanism. The effects of ionospheric scintillation include a transient increase in errors of the carrier phase and code measurements, which might cause the PLL tracking loop to get out of the lock stage if they exceed the threshold value[16-18]. For example, W. Chen, et al. [19] reported that the strong ionospheric scintillation caused by strong solar activities had once induced a large number of lock losses and increased phase measurement noises. The multipath signals also bring irregular phase errors in the GPS measurements[20]. Thus, to tackle these problems, an optimal-state-estimation-based PLL is needed, which enhances the PLL performances by estimating the difference of the optimal carrier phase and the Doppler frequency shift between the actual and the local signals.

The three-state dynamic model of a discrete-time reconstructed carrier has been developed. In the processing period of T_{k-1} to T_k, it can be formulated as[6, 14]

$$\begin{bmatrix} x_{\mathrm{p}} \\ x_{\mathrm{v}} \\ x_{\mathrm{a}} \end{bmatrix}_k = \begin{bmatrix} 1 & \Delta T & \dfrac{\Delta T^2}{2} \\ 0 & 1 & \Delta T \\ 0 & 0 & 1 \end{bmatrix} \begin{bmatrix} x_{\mathrm{p}} \\ x_{\mathrm{v}} \\ x_{\mathrm{a}} \end{bmatrix}_{k-1} + \begin{bmatrix} -\Delta T \\ 0 \\ 0 \end{bmatrix} \omega_{\mathrm{re}(k-1)} + \begin{bmatrix} 1 & 0 & 0 \\ 0 & 1 & 0 \\ 0 & 0 & 1 \end{bmatrix} \boldsymbol{w}_{k-1} \tag{10}$$

where ΔT is the processing time interval of the tracking loop, $\omega_{\mathrm{re}(k-1)}$ the nominal Doppler shift of the local generated carrier, x_{p} the carrier phase difference between the received signal and the local reconstructed signal, x_{v} the Doppler frequency of the received carrier signal, x_{a} the drift rate of the Doppler shift, $\boldsymbol{w}_{\mathrm{k}}$ represents white, zero-mean Gaussian random sequences:

$$E(\boldsymbol{w}_k) = \boldsymbol{0}$$
$$E(\boldsymbol{w}_k \boldsymbol{w}_k^{\mathrm{T}}) = \boldsymbol{Q}_k$$

The measured $\boldsymbol{z}_{\mathrm{k}}$ is obtained directly from the phase discriminator and calculated using PLL's in-phase and quadrature accumulations. Over one measurement period, it can be linearly expressed in terms of state variations as[14]

$$\boldsymbol{z}_k = \frac{1}{\Delta T}\int_{t_{k-1}}^{t_k} x_p(t)\mathrm{d}t + \boldsymbol{v}_k = \begin{bmatrix} 1 & \dfrac{\Delta T}{2} & \dfrac{\Delta T^2}{6} \end{bmatrix} \begin{bmatrix} x_{\mathrm{p}} \\ x_{\mathrm{v}} \\ x_{\mathrm{a}} \end{bmatrix}_{k-1} - \frac{\Delta T}{2}\omega_{re(k-1)} + \begin{bmatrix} 1 & 0 & 0 \end{bmatrix} \boldsymbol{w}_{(k-1)} + \boldsymbol{v}_k \tag{11}$$

where $\boldsymbol{v}_{\mathrm{k}}$ is white, zero-mean Gaussian random sequence:

$$E(\boldsymbol{v}_k) = \boldsymbol{0}$$
$$E(\boldsymbol{v}_k \boldsymbol{v}_k^{\mathrm{T}}) = \boldsymbol{R}_k$$

Then, the linear dynamic model in Eq.(10) and Eq.(11) can be expressed in a standard matrix-vector form as follows:

$$\boldsymbol{x}_k = \boldsymbol{\Phi}_{k,k-1}\boldsymbol{x}_{k-1} + \boldsymbol{B}_{k-1}\boldsymbol{u}_{k-1} + \boldsymbol{\Gamma}_{k-1}\boldsymbol{w}_{k-1} \tag{12}$$

$$\boldsymbol{z}_k = \boldsymbol{H}_{k-1}\boldsymbol{x}_{k-1} + \boldsymbol{y}_{k-1} + \boldsymbol{v}_k^* \tag{13}$$

where

$$\left.\begin{aligned} \boldsymbol{\Phi}_{k,k-1} &= \begin{bmatrix} 1 & \Delta T & \dfrac{\Delta T^2}{2} \\ 0 & 1 & \Delta T \\ 0 & 0 & 1 \end{bmatrix} \\ \boldsymbol{B}_{k-1}\boldsymbol{u}_{k-1} &= \begin{bmatrix} -\Delta T \\ 0 \\ 0 \end{bmatrix} \omega_{re_{(k-1)}} \end{aligned}\right\} \tag{14}$$

$$\left.\begin{aligned} \boldsymbol{y}_{k-1} &= -\frac{\Delta T}{2}\omega_{\mathrm{re}_{(k-1)}} \\ \boldsymbol{v}_k^* &= \begin{bmatrix} 1 & 0 & 0 \end{bmatrix} \boldsymbol{w}_{(k-1)} + \boldsymbol{v}_k \end{aligned}\right\} \tag{15}$$

Here, $\boldsymbol{u}_{\mathrm{k-1}}$ and $\boldsymbol{y}_{\mathrm{k-1}}$ can be considered as controlled variables. $\boldsymbol{w}_k$ in Eq.(12) is the input disturbance, and $\boldsymbol{v}_k^*$ the measurement noise. Both of them are white, zero-mean Gaussian random sequences. Apparently, from Eq.(15), they are cross- correlated with the following covariance:

$$\mathrm{Cov}(\boldsymbol{w}_k, \boldsymbol{v}_k^*) = \boldsymbol{S}_k\delta_k \tag{16}$$

As the foundation of a linear minimum-variance estimation requires to be without cross-correlated noises, Eq. (12) and Eq. (13) must be de-correlated firstly.

By adding a new zero-equivalent item $(\boldsymbol{J}_{k-1} \cdot (\boldsymbol{z}_{k-1} - \boldsymbol{H}_{k-1}\boldsymbol{x}_{k-1} - \boldsymbol{y}_{k-1} - \boldsymbol{v}_{k-1}^*))$ on the right of Eq.(12), can be obtained

$$\boldsymbol{x}_k = \boldsymbol{\Phi}_{k,k-1}\boldsymbol{x}_{k-1} + \boldsymbol{B}_{k-1}\boldsymbol{u}_{k-1} + \boldsymbol{\Gamma}_{k-1}\boldsymbol{w}_{k-1} + \boldsymbol{J}_{k-1}(\boldsymbol{z}_{k-1} - \boldsymbol{H}_{k-1}\boldsymbol{x}_{k-1} - \boldsymbol{y}_{k-1} - \boldsymbol{v}_{k-1}^*) \tag{17}$$

where $\boldsymbol{J}_{\mathrm{k-1}}$ is an unknown matrix to be determined. Then a new transition matrix and a new input distur-

bance can be written into

$$\boldsymbol{\Phi}^*_{k,k-1} = \boldsymbol{\Phi}_{k,k-1} - \boldsymbol{J}_{k-1}\boldsymbol{H}_{k-1} \tag{18}$$

$$\boldsymbol{w}^*_{k-1} = \boldsymbol{\Gamma}_{k-1}\boldsymbol{w}_{k-1} - \boldsymbol{J}_{k-1}\boldsymbol{v}^*_{k-1} \tag{19}$$

Eq. (17) can be rewritten into

$$\boldsymbol{x}_k = \boldsymbol{\Phi}^*_{k,k-1}\boldsymbol{x}_{k-1} + \boldsymbol{B}_{k-1}\boldsymbol{u}_{k-1} + \boldsymbol{J}_{k-1}(\boldsymbol{z}_{k-1} - \boldsymbol{y}_{k-1}) + \boldsymbol{w}^*_{k-1} \tag{20}$$

Then the covariance between $\boldsymbol{w}^*_k$ and $\boldsymbol{v}^*_k$ can be calculated by substituting Eq.(15) and Eq.(19) into the following equation:

$$\mathrm{Cov}(\boldsymbol{w}^*_k, \boldsymbol{v}^*_k) = E(\boldsymbol{\Gamma}_k\boldsymbol{w}_k - \boldsymbol{J}_k\boldsymbol{v}^*_k)\boldsymbol{v}^{*\mathrm{T}}_k = (\boldsymbol{\Gamma}_k\boldsymbol{S}_k - \boldsymbol{J}_k\boldsymbol{R}_k)\delta_k \tag{21}$$

From Eq.(21), in order to make $\mathrm{Cov}(\boldsymbol{w}^*_k, \boldsymbol{v}^*_k) = 0$, the unknown matrix $\boldsymbol{J}_k$ must be valued by $\boldsymbol{J}_k = \boldsymbol{\Gamma}_k\boldsymbol{S}_k\boldsymbol{R}_k^{-1}$.

Under this condition, the input disturbance $\boldsymbol{w}^*_k$ and the measurement noise $\boldsymbol{v}^*_k$ become no longer cross-correlated in the new expression, and thus Eq.(20) and Eq.(13) constitute a standard linear dynamic discrete-time model. Based on the projection theory, the optimal linear estimator can be deduced as follows.

First, make the state estimate prediction by

$$\hat{\boldsymbol{x}}_{k,k-1} = \boldsymbol{\Phi}^*_{k,k-1}\hat{\boldsymbol{x}}_{k-1} + \boldsymbol{B}_{k-1}\boldsymbol{u}_{k-1} + \boldsymbol{J}_{k-1}(\boldsymbol{z}_{k-1} - \boldsymbol{y}_{k-1}) \tag{22}$$

Then, compute the optimal state estimates by

$$\hat{\boldsymbol{x}}_k = \hat{\boldsymbol{x}}_{k,k-1} + \boldsymbol{K}_k(\boldsymbol{z}_k - \boldsymbol{y}_k - \boldsymbol{H}_k\hat{\boldsymbol{x}}_{k,k-1}) \tag{23}$$

where $\boldsymbol{K}_k$ is the optimal Kalman filter gain. The state estimate error can be described by

$$\boldsymbol{\varepsilon}_k = \hat{\boldsymbol{x}}_k - \boldsymbol{x}_k \tag{24}$$

Then the covariance of the state estimate error can be expressed by

$$\begin{aligned}\boldsymbol{P}_k = E[\varepsilon_k\varepsilon_k^{\mathrm{T}}] = \\ \boldsymbol{P}_{k,k-1} - \boldsymbol{P}_{k,k-1}\boldsymbol{H}_k^{\mathrm{T}}(\boldsymbol{H}_k\boldsymbol{P}_{k,k-1}\boldsymbol{H}_k^{\mathrm{T}} + \boldsymbol{R}_k)^{-1}\cdot \\ \boldsymbol{H}_k\boldsymbol{P}_{k,k-1} + [\boldsymbol{K}_k - \boldsymbol{P}_{k,k-1}\boldsymbol{H}_k^{\mathrm{T}}(\boldsymbol{H}_k\boldsymbol{P}_{k,k-1}\boldsymbol{H}_k^{T} + \\ \boldsymbol{R}_k)^{-1}](\boldsymbol{H}_k\boldsymbol{P}_{k,k-1}\boldsymbol{H}_k + \boldsymbol{R}_k)\cdot \\ [\boldsymbol{K}_k - \boldsymbol{P}_{k,k-1}\boldsymbol{H}_k^{\mathrm{T}}(\boldsymbol{H}_k\boldsymbol{P}_{k,k-1}\boldsymbol{H}_k^{\mathrm{T}} + \boldsymbol{R}_k)^{-1}]\end{aligned} \tag{25}$$

The optimal gain matrix is obtained by minimizing the expected value of the state error covariance ($\boldsymbol{P}_k$) at each step, hence the following cost function is to be minimized by the choice of $\boldsymbol{K}_k$. The minimum value can be attained when

$$\frac{\partial P_k}{\partial K_k} = 0 \tag{26}$$

Substituting Eq.(25) into Eq.(26), the optimal gain can be obtained as

$$\boldsymbol{K}_k = \boldsymbol{P}_{k,k-1}\boldsymbol{H}_k^{\mathrm{T}}(\boldsymbol{H}_k\boldsymbol{P}_{k,k-1}\boldsymbol{H}_k^{\mathrm{T}} + \boldsymbol{R}_k)^{-1} \tag{27}$$

Then the optimal state error covariance $\boldsymbol{P}_k$ can be rewritten into

$$\boldsymbol{P}_k = \boldsymbol{P}_{k,k-1} - \boldsymbol{P}_{k,k-1}\boldsymbol{H}_k^{\mathrm{T}}(\boldsymbol{H}_k\boldsymbol{P}_{k,k-1}\boldsymbol{H}_k^{\mathrm{T}} + \boldsymbol{R}_k)^{-1}\boldsymbol{H}_k\boldsymbol{P}_{k,k-1} = (\boldsymbol{I} - \boldsymbol{K}_k\boldsymbol{H}_k)\boldsymbol{P}_{k,k-1} \tag{28}$$

In the same way, the covariance of the state error before the measurement update (predicted estimate covariance) is described by

$$\boldsymbol{\varepsilon}_{k,k-1} = \hat{\boldsymbol{x}}_{k,k-1} - \boldsymbol{x}_k \tag{29}$$

$$\begin{aligned}\boldsymbol{P}_{k,k-1} = E[\boldsymbol{\varepsilon}_{k,k-1}\boldsymbol{\varepsilon}_{k,k-1}^{\mathrm{T}}] = \\ \boldsymbol{\Phi}^*_{k,k-1}\boldsymbol{P}_{k-1}\boldsymbol{\Phi}^{*\mathrm{T}}_{k,k-1} + E(\boldsymbol{w}^*_{k-1}\boldsymbol{w}^{*\mathrm{T}}_{k-1}) = \\ (\boldsymbol{\Phi}_{k,k-1} - \boldsymbol{J}_{k-1}\boldsymbol{H}_{k-1})\boldsymbol{P}_{k-1}(\boldsymbol{\Phi}_{k,k-1} - \\ \boldsymbol{J}_{k-1}\boldsymbol{H}_{k-1})^{\mathrm{T}} + \boldsymbol{\Gamma}_{k-1}\boldsymbol{Q}_{k-1}\boldsymbol{\Gamma}_{k-1}^{\mathrm{T}} - \boldsymbol{J}_{k-1}\boldsymbol{R}_{k-1}\boldsymbol{J}_{k-1}^{\mathrm{T}}\end{aligned} \tag{30}$$

To sum up, the five Equations to set up a standard Kalman filter are listed as below:

For prediction:

$$\hat{\boldsymbol{x}}_{k,k-1} = \boldsymbol{\Phi}^*_{k,k-1}\hat{\boldsymbol{x}}_{k-1} + \boldsymbol{B}_{k-1}\boldsymbol{u}_{k-1} + \boldsymbol{J}_{k-1}(\boldsymbol{z}_{k-1} - \boldsymbol{y}_{k-1}) \tag{31}$$

$$\begin{aligned}\boldsymbol{P}_{k,k-1} = (\boldsymbol{\Phi}_{k,k-1} - \boldsymbol{J}_{k-1}\boldsymbol{H}_{k-1})\boldsymbol{P}_{k-1}\cdot \\ (\boldsymbol{\Phi}_{k,k-1} - \boldsymbol{J}_{k-1}\boldsymbol{H}_{k-1})^{\mathrm{T}} + \\ \boldsymbol{\Gamma}_{k-1}\boldsymbol{Q}_{k-1}\boldsymbol{\Gamma}_{k-1}^{\mathrm{T}} - \boldsymbol{J}_{k-1}\boldsymbol{R}_{k-1}\boldsymbol{J}_{k-1}^{\mathrm{T}}\end{aligned} \tag{32}$$

For estimation:

$$\boldsymbol{K}_k = \boldsymbol{P}_{k,k-1}\boldsymbol{H}_k^{\mathrm{T}}(\boldsymbol{H}_k\boldsymbol{P}_{k,k-1}\boldsymbol{H}_k^{\mathrm{T}} + \boldsymbol{R}_k)^{-1} \tag{33}$$

$$\hat{\boldsymbol{x}}_k = \hat{\boldsymbol{x}}_{k,k-1} + \boldsymbol{K}_k(\boldsymbol{z}_k - \boldsymbol{y}_k - \boldsymbol{H}_k\hat{\boldsymbol{x}}_{k,k-1}) \tag{34}$$

$$\boldsymbol{P}_k = (\boldsymbol{I} - \boldsymbol{K}_k\boldsymbol{H}_k)\boldsymbol{P}_{k,k-1} \tag{35}$$

4. Verification Results

To evaluate the performances of the proposed PLL algorithm, the NAMURU V2 GPS data logging board is used to collect the real IF signals. Fig.3 shows the software receiver platform. The IF frequency is 1.405 396 MHz and the sampling rate is 5.714 286 MHz. This verification uses two sets of data separately sampled from the roof of Hong Kong Polytechnic University and indoor site by windows tightly encircled by tall concrete buildings vulnerable to strong effects of phase jitters as is expected. With the purpose of making comparison of the performances, the same data are processed with both traditional second-order PLL described in Section 2 (with the optimal noise bandwidth of 7.65 Hz and the damping factor of 0.7[21]) and a PLL-based Kalman filter proposed in Section 3.

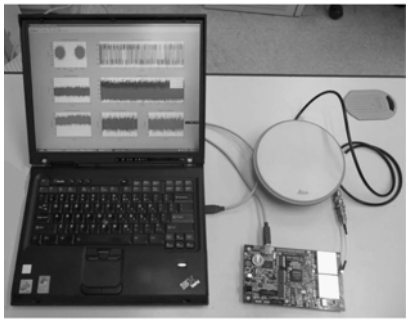

Fig.3 A GPS software receiver platform.

4.1. Normal GPS signal processing

The sampled data used in this processing are from satellite PRN 21, and registered in an opening area with the nominal C/N_0 of 42 dB-Hz. According to a large amount of statistical data on GPS signal noise, the noise covariance Q is chosen to be diag [4.84 $\times 10^{-4}$ (cycle)^2, 8.523$\times 10^{-3}$ (Hz)^2, 0.864$\times 10^{-3}$ (Hz/s)^2] and the measurement covariance $\boldsymbol{R}$ is [1.03$\times 10^{-3}$ (cycle)^2]. Fig.4 compares the performances of the traditional second-order PLL and the new Kalman-filter-based PLL in terms of phase errors and Fig.5 in terms of Doppler frequency shifts. From Fig.4, it can be observed that the standard deviation is 0.01069 cycle for the second-order PLL and 0.007 63 cycle for the Kalman-filter-based PLL. Clearly, the performance of the Kalman-based-PLL is significantly better than the traditional second-order PLL. This improvement is more highlighted by Fig.5 in terms of the Doppler shift estimation meaning the Kalman-based-PLL causes less overshot and takes shorter converge time.

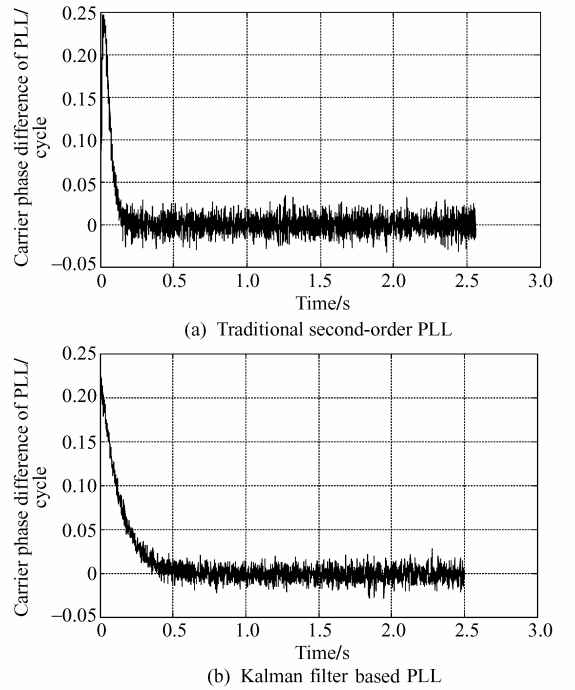

Fig.4 Comparison of performances between traditional second-order PLL and Kalman-filter-based PLL in terms of phase errors.

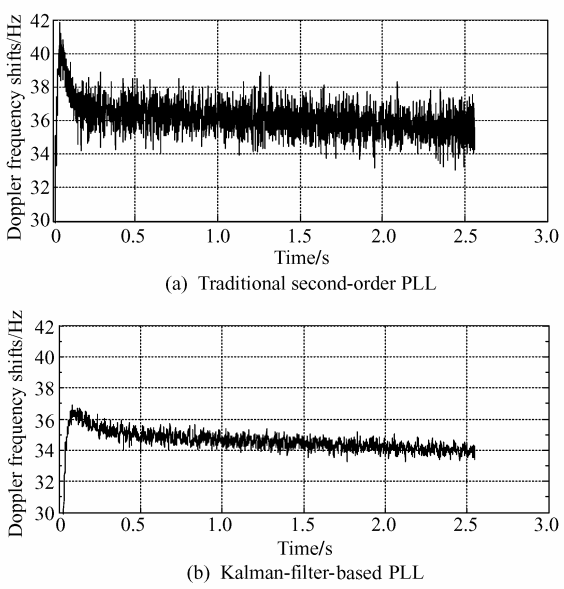

Fig.5 Comparison of performances between traditional second-order PLL and Kalman-filter-based PLL in terms of Doppler frequency shifts.

4.2. Weak GPS signal processing

In order to estimate the realtime C/N_0 of the received signals, this article uses the method of adding noise channel[22]. Fig.6 shows the changes of C/N_0 of the weak GPS signals sampled in this test against the time. The lowest C/N_0 of about 26dB-Hz during 3-13 s, the worst C/N_0 condition period during processing, speaks volume about the effectiveness of this improved PLL (see Fig.6). Fig.7 compares the performances between the traditional second-order PLL and the Kalman-filter-based PLL in terms of phase errors and Fig.8 in terms of frequency shifts both during processing weak signals. From Fig.7(a) and Fig.8(a), a series of transient phase jitter errors can be discovered in the traditional second-order processed results (during 2-6 s). This phase jitter ranges between about ±25° (Fig.7 (a)), which corresponds to Doppler shifts of ±15 Hz (see Fig.8(a)). However, Fig.7(b) and Fig.8(b) evince remarkable advances that the Kalman-filter-based PLL has made by reducing the phase jitter range to ±17° and the Doppler shift to ±5 Hz. This is because when a transient phase jitter occurs, the improved PLL could make correct estimation of the next carrier phase thereby keeping

an effective check on the transient jitter and resulting in less noise disturbance.

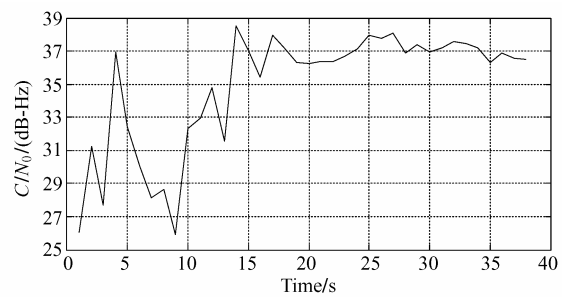

Fig.6 Realtime C/N_0 estimation of received signals.

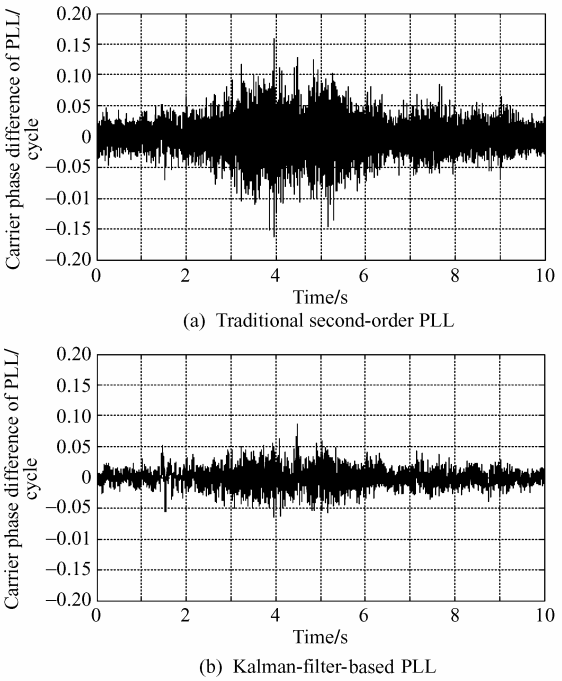

Fig.7 Comparison of performances between traditional second-order PLL and Kalman-filter-based PLL in terms of phase errors for processing weak signals.

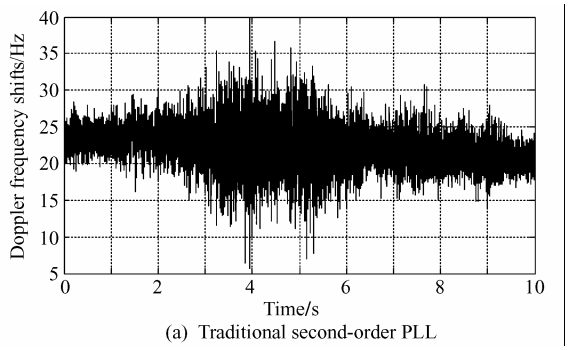

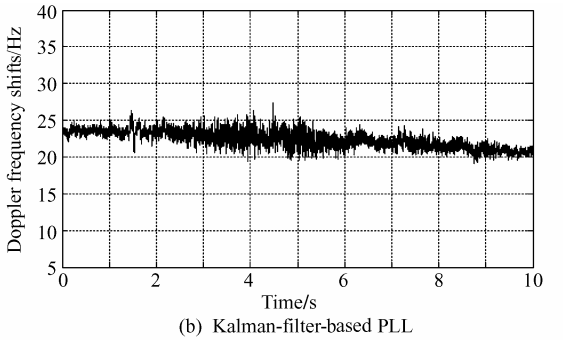

Fig.8 Comparison of performances between traditional second-order PLL and Kalman-filter-based PLL in terms of Doppler frequency shifts for processing weak signals.

5. Conclusions

This article proposes and analyzes an improved Kalman-filter-based PLL for processing weak carrier signals. Compared with the traditional second-order PLL, this new PLL is able to suppress the transient irregular phase jitter noises by estimating the optimal phase errors. This improves that PLL for tracking weak GPS signals has been validated against real digital data gathered in real circumstances with weak signals. Results prove the essential improvements which the proposed PLL brought about in tracking weak GPS signals.

References

[1] Akos D M. A software radio approach to global navigation satellite system receiver design. PhD thesis, School of Elect, Ohio University, 1997.

[2] Morton Y, Tsui J, Lin D, et al. Assessment and handling of CA code self-interference during weak GPS signal acquisition. Proceedings of ION GPS 2003. 2003; 646-653.

[3] Tsui J B. Fundamentals of global positioning system receivers:a software approach. 2nd ed. New York: Wiley & Sons, 2005.

[4] Kaplan E D. Understanding GPS, principles and applications. 2nd ed. Boston: Artech House, Inc., 2006.

[5] Psiaki M L. Block acquisition of weak GPS signals in a software receiver. Proceedings of ION GPS 2001. 2001; 2838-2850.

[6] Liao B Y, Hong Y, Lin B J. Smoother and Bayesian filter based semi-codeless tracking of dual-frequency GPS signals. Science in China (Series F): Information Sciences 2006; 49(4): 533-544.

[7] Ziedan N I, Garrison J L. Extended Kalman filter-based tracking of weak GPS signals under high dynamic conditions. Proceedings of ION GNSS 2004. 2004; 20-31.

[8] Razavi A, Gebre-Egziabher D, Akos D M. Carrier loop architectures for tracking weak GPS signals. IEEE Transactions on Aerospace and Electronic Systems 2008; 44(2):697-710.

[9] Legrand F, Macabiau C. Improvement of pseudo-

range measurements accuracy by using fast adaptive bandwidth lock loops. Proceedings of ION GPS 2000. 2000; 2346-2356.
[10] Townsend B, Fenton P, Dierendonck K V, et al. L1 carrier phase multipath reduction using MEDLL technology. Proceedings of ION GPS 1995. 1995; 1539-1544.
[11] Bhuiyan M Z H, Lohan E S, Renfors M. Code tracking algorithms for mitigating multipath effects in fading channels for satellite-based positioning. EURASIP Journal on Advances in Signal Processing 2008; Article ID 863629, doi:10. 1155/2008/863629.
[12] Soloviev A, Van Graas F, Gunawardena A. Implementation of deeply integrated GPS/low-cost IMU for acquisition and tracking of low CNR GPS signals. Proceedings of ION National Technical Meeting. 2004; 923-936.
[13] Razavi A. Sensitivity and performance analysis of doppler aided GPS carrier tracking loops. PhD thesis, Department of Electrical and Computer Engineering, University of Minnesota, 2004.
[14] Psiaki M L. Attitude sensing using a global-positioning-system antenna on a turntable. Journal of Guidance, Control, and Dynamics 2000; 24(1): 474-481.
[15] Psiaki M L. Smoother-based GPS signal tracking in a software receiver. Proceedings of ION GPS 2001. 2001; 2900-2913.
[16] Yu W, Lachappelle G, Skone S. PLL performance for signals in the presence of thermal noise, phase noise, and ionospheric scintillation. Proceedings of ION GNSS 2006. 2006; 1341-1357.
[17] Conker R S, El-Arini M, Hegarty C, et al. Modeling the effects of ionospheric scintillation on GPS/satellite-based augmentation system availability. Radio Sci 2003; 38(1):1-23.
[18] Kondo S, Ebinuma T, Kubo N, et al. Evaluation of tracking performance in the presence of ionospheric scintillation on GPS signal in Japan. Proceedings of ION GNSS 2007. 2007; 2832-2839.
[19] Chen W, Gao S, Hu C W, et al. Effects of ionospheric disturbances on GPS observation in low latitude area. GPS Solutions 2008; 12(1):33-41.
[20] Ray J K, Cannon M E, Fenton P. GPS code and carrier multipath mitigation using a multiantenna system. IEEE Transactions on Aerospace and Electronic Systems 2001; 37(1):183-195.
[21] Borre K, Akos D M, Bertelsen N, et al. A software-defined GPS and Galileo receiver:a single-frequency approach. Boston:Birkhuser, 2007.
[22] Tang X M. Carrier recovery and carrier to noise estimation in high-quality navigation receiver. Master thesis, School of Information and Communication Engineering, National University of Defense Technology, 2005. [in Chinese]

Biography:

Miao Jianfeng Born in 1981, he received B. S. degree from Nanjing University of Aeronautics and Astronautics (NUAA) in 2004, and then became a Ph.D. candidate under the joint supervision Ph. D. scheme of NUAA and Hong Kong Polytechnic University. His main research interests are GPS software receiver and navigation system.
E-mail: dbqr@163.com